http://doi.org/10.1590/jatm.v16.1337 ORIGINAL PAPER

Experimental and Numerical Investigation of the Natural Frequency for the Intact and Cracked Laminated Composite Beam

Raghad Azeez Neamah[1,*], Saddam Khalsan Al-Raheem[1], Emad Kadum Njim[2], Zainab Abboud[3], Luay Sadeq Al-Ansari[1]

1. University of Kufa – Faculty of Engineering – Department of Mechanical Engineering – Najaf – Iraq.
2. Ministry of Industry and Minerals – State Company for Rubber and Tires Industries – Najaf – Iraq.
3. AL-Furat Al-Awsat Technical University – Faculty of Kufa Institute – Kufa – Iraq.

*Correspondence author: ragada.deibel@uokufa.edu.iq

ABSTRACT

In this study, several composite beam samples were made from woven fiberglass and epoxy. The first sample was created using epoxy, whereas the others used epoxy together with fiberglass layers. These samples were used to study, experimentally and numerically, the effect of fiberglass layers on the natural frequency of composite beams. A numerical model was constructed using ANSYS software 17.2 to assess vibration properties for the manufactured samples. The effects of boundary conditions (simply supported, clamped-clamped, and clamped-free), with crack depths (2 mm and 3 mm) and the number of fiberglass layers (0, 1, 2, 3, and 4) were investigated. The results of the experimental and numerical models were compared, and the numerical model was acceptable with an error rate of less than 15%. Crack depth has a significant impact on natural frequency and mode shape; therefore, transverse cracks were created in the upper surfaces of beams to investigate the vibration mode shape and natural frequency.

Keywords: Frequency; Cracked composite beam; Fiberglass; Epoxy; Free vibration; Mode shape.

INTRODUCTION

A composite material is created by combining two or more materials having dissimilar physical and chemical characteristics to create a new material with better qualities. The components of a composite material can have various chemical properties and not be soluble or fusible with one another (Tri-Dung 2020). Resin serves as the matrix for the polymer composite, and fibers act as reinforcement. Due to its advantageous qualities at room temperature, simplicity in manufacture, and cost-effectiveness, this material is widely used in a variety of applications. The many categories of polymer matrix composites (PMCs) depend on the kind of reinforcement, such glass and carbon fibers. Additionally, other polymer resins, such as epoxy and phenolic resins, are used. Fiberglass is used in industrial floors, pipelines, containers, and the automotive and marine industries (Dipen *et al.* 2021). In the last few decades, there has been significant interest in investigating the use of natural fibers such as banana, straw, hemp, jute, and flax as reinforcements in materials (Reddy *et al.* 2021; Sanjay *et al.* 2014). However, the most promising results to date have been achieved using polyester and certain phenolic resins as reinforcements (Libo *et al.* 2014; Weronika *et al.* 2023). Another extensively studied issue is the weathering behavior of natural fiber-reinforced composites, including investigating the water sorption effect on the mechanical properties of laminate (Suriani *et al.* 2021).

Received: Sep 02 2023 | **Accepted:** May 23 2024
Section editor: Renato Rebouças de Medeiros
Peer Review History: Single Blind Peer Review.

Many studies deal with the vibration effect on cracked and intact composite beams. For example, Daneshmehr *et al.* (2013) applied the first shear deformation theory to analyze the vibration of cracked composite beams exposed to torsion loading. The effect of shear deformation and crack depth on natural frequency was studied numerically. Jena *et al.* (2014) presented theoretical, experimental, and numerical methods to analyze the free vibration of cracked fiber composite beams. The effect of crack position and boundary conditions on natural frequency is studied. Orhan *et al.* (2016) examined the depth influence of V-shaped cracks on the frequency of cantilever composite beams experimentally and then numerically. Naskar *et al.* (2017) presented the approach of a stochastic approach to the free vibration of thin-walled cracked laminated composite beams. Kahya *et al.* (2019) used a shear-deformable 13 degrees of freedom numerical model to evaluate the free vibration of a laminated composite beam. Kim *et al.* (2019) used the Ritz method and first shear deformation theory to evaluate the vibration behavior of a rectangular cross-section laminated composite beam with a crack. Kahya *et al.* (2021) used vibration measurements to present the localization and identification of the transverse edge cracks in laminated composite beams. Sahu and Das (2020) studied the natural frequencies of a symmetrically laminated beam with transverse open cracks by using the first shear deformation theory with different boundary conditions. Das and Sahu (2020) determined numerically and experimentally how crack depth and position affected the natural frequency of laminated beams. Du *et al.* (2023) studied the flexural properties of high-strength steel-concrete composite beans using bending tests and analyzed the effect of concrete strength on the failure mode and load deflection behavior. Priyadarshi *et al.* (2021) studied, experimentally, the transverse crack detection woven fiber laminated glass-epoxy composite beams using different vibration modes of natural frequencies and employing a "Mamdani hybrid fuzzy logic inference system (FIS)". They also the finite element method (FEM) to analyze the same problem using Abaqus software. They studied the effect of crack position and crack depth. They found that the hybrid FIS closely resembled the experimental analysis and was an effective method for crack detection in laminated composite beam (LCB) over other standalone methods. Considering a linear beam model, Priyadarshi and Shishir (2021) used the finite element technique to investigate the impacts of ply number, lamination scheme, ply-orientation, and aspect ratios with various support types on the natural frequencies of "industry-driven woven fiber laminated carbon/epoxy composite beams" using Abaqus software. Additionally, they used a fast Fourier transform (FFT) analyzer to measure the natural frequencies. They found that "the predicted vibration characteristics of laminated composite beams are sensitive to the adopted parameters for the investigation". Priyadarshi and Shishir (2022) modified their work by applying finite element predictions were made using the MATLAB platform by developing a programmable computer code accounting for shear deformation. They concluded that "the free-vibration finite element predictions for glass/epoxy beams are sensitive to effects of different boundary conditions and span-to-thickness ratios".

Hu *et al.* (2023) analyzed the free vibration of the cracked thick plates with different boundary conditions (simply supported [S-S] and clamped edge). Zou *et al.* (2023), based on the mechanical properties of fiber-reinforced polymer materials, proposed a new structure for the web-concrete composite T-beam to solve the conventional problems of heavyweight and web cracking. Priyadarshi *et al.* (2024) investigated the impacts of transverse open cracks on the dynamic characteristics of "woven fiber LCB" using a FFT analyzer system and Abaqus software. They studied the impacts of several parameters such as relative crack depth and crack location, in addition to fiber orientations and support types, on the frequency of the cracked LCB. Their results showed that "the maximum decrease in frequencies is observed for 0° ply oriented single and multi-cracked LCB".

The expansion of early cracks is the most common cause of failure in dynamically loaded beams. As a result, it is critical to explore crack propagation analysis and testing on a composite beam. The free vibration of a new model for cracked and intact composite beams is computationally and empirically investigated in this paper. The ANSYS-APDL software 17.2 is used to compute the natural frequency of these beams and shows their first-mode form, while the epoxy and fiberglass materials are employed to make these beams to assess their natural frequency and increase the validity of the numerical model. The influence of the number of fiberglass layers, boundary conditions, and crack depths is investigated numerically and experimentally.

Experimental work

The experimental study included the creation of composite beams with epoxy and varying quantities of fiberglass layers based on volume fraction percentages.

Materials used and mechanical properties

The materials used in this work, along with their properties, are presented in Table 1 (Gay 2022; Shareef *et al.* 2021).

Table 1. Mechanical properties of E-glass fibers and Quick mast 105 epoxy.

Mechanical property	E-glass fibers	Epoxy	Unit
Density	2.600	1.150	Kg·m^3
Tensile strength	2.5	0.028	GPa.
Modulus of elasticity E	74	0.6157	GPa.
Poisson ratio)ν(	0.25	0.33	-

Source: Gay (2022) and Shareef *et al.* (2021).

Designing and manufacturing the composite beam

The composite beams were created using glass molds. These beams were constructed using epoxy and various volume fractions of E-glass fibers. Each layer's volume can be estimated using its mass and density. The volume fraction of each fiber layer (V_f) is then computed, as shown in Table 2, by dividing its volume by the overall volume of the mold. The Eqs. 1-3 were used to perform the calculations:

$$V_{mold} = \text{Thickness} \cdot \text{Width} \cdot \text{Length} = 0.4 \cdot 8 \cdot 14 = 44.8 \text{ cm}^3 \quad (1)$$

$$V = \frac{m_{E-glass}}{\rho_{E-glass}} \quad (2)$$

where: $\rho_{E\text{-}glass} = 2.6\text{g/cm}^3$; $m_{E\text{-}glass} = 5\text{g}$

$$(V_f)_{\text{E-glass}} = \frac{V}{V_{mold}} \quad (3)$$

Table 2. Volume fraction of the manufactured beams.

Volume of mold	Number of E-glass layers	Volume of epoxy (cm^3)	Volume of E-glass (cm^3)	Volume fraction of E-glass (%)
44.8	Zero	44.8	0	0
	One layer	42.877	1.923	4.29
	Two layers	40.954	3.846	8.58
	Three layers	39.031	5.769	12.87
	Four layers	37.108	7.692	17.169

Source: Elaborated by the authors.

After calculating the volume fraction of each of epoxy and fiberglass, the next steps of production are presented: 1) manufacturing of glass molds with dimensions of 14 cm length, 8 cm width, and 0.4 cm thickness, as shown in Fig. 1a; 2) weighing (one, two, three, and four layers) of fiberglass that used as reinforced material, as shown in Fig. 1b; 3) lubricating the mold and putting a tube inside to inject the epoxy, as shown in Fig. 1a-c; 4) closing the mold and then mixing and injecting epoxy, as shown in Fig. 1d and f; 5) removing the sample from the mold and then cutting it into the shape of a beam by computer numerical control (CNC) machine with dimensions of 12 cm length, 1 cm width, and 0.4 cm thickness, as shown in Fig. 1g; 6) making cracks on the top surface of these beams with different depths, as shown in Fig. 1h; 7) measuring the natural frequency of the intact and cracked beams using free vibration test.

The free vibration test

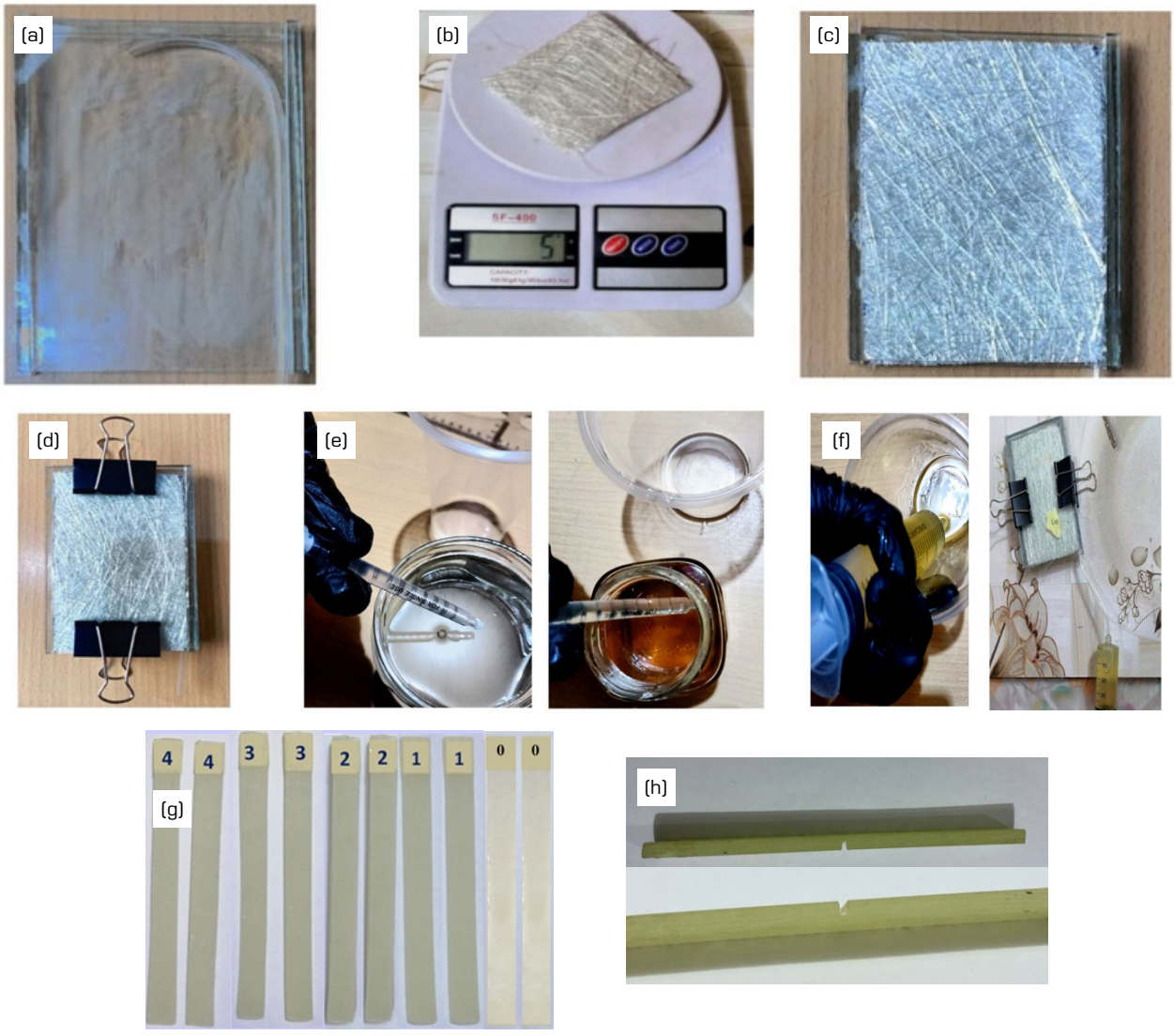

Source: Elaborated by the authors.

Figure 1. Steps for manufacturing the composite beam samples. (a) glass mold and feeding tube inserting; (b) layer weighting; (c) layer of fiberglass; (d) close the mold; (e) mixing the epoxy and hardener; (f) injuction the epoxy resin; (g) composite beams; (h) crack's shape.

The natural frequency is measured using the vibration structure rig. This rig consists of the following components, as illustrated in Fig. 2a: a) Impact hammer, model (086C03) (PCB Piezotronics vibration division), with the information about measurement range (22.24 N), resonant frequency (≥ 22 kHz), excitation voltage (20 to 30 VDC), constant current excitation (2 to 20 mA), output bias voltage (8 to 14 VDC), discharge time constant (≥ 2000 sec), hammer mass (0.16 kg), head diameter (1.57 cm), tip diameter (0.63 cm), and hammer length (21.6 cm). Impulse force test hammer is adapted for adapts FFT analysis of structure behavior testing. Impulse testing of the dynamic behavior of mechanical structure involves striking the test object with the force-instrumented hammer, and measuring the resultant motion with an accelerometer; b) Accelerometer, model (SN 151779), with the information, lower frequency (determined by the amplifier used), upper frequency limit (+ 10%) (12.6 kHz), mounted resonance frequency (42 kHz), and weight (11 g). c) amplifier, model 480E09, the amplifier measures the response signal from accelerometer and gives output signal to the digital storage oscilloscope; d) digital storage oscilloscope, model ADS

1202CL+, and the serial no. 01020200300012, with the information maximum frequency (200 MHz) and maximum read of sample per second (500 MSa·s).

The following steps were used to achieve the vibration test for measuring the natural frequency of beam: 1) support the beam as a clamped-free (C-F) supported beam (Fig. 2b); 2) impact the C-F beam at the free end using the impact hammer (Fig. 2c); 3) save the vibration signal obtained from accelerometer used the removable disc; 4) transfer the vibration signal from time domain to frequency domain (Fig. 2d) by applying FFT using sig-view software in order to find the natural frequency.

Numerical method

The natural frequency of homogeneous and composite beams with and without cracks is calculated using the ANSYS APDL 17.2 program. The composite beam is made up of epoxy plus one, two, three, or four layers of E-glass fiber in the thickness direction, compared to the homogeneous beam, which is formed just of epoxy. The dimensions of this beam are 12 cm in length, 1 cm in width, and 0.4 cm in thickness. A crack in the composite beam is created on the top surface of the beam with varied depths (2 and 3 mm) in the thickness direction, as shown in Fig. 3, to investigate the effect of boundary conditions, the number of fiberglass layers, and crack depths. Table 1 presents the mechanical properties required, such as density, Poisson's ratio, and elastic modulus. The solid-type tetrahedral 10-node 187 is chosen for meshing because it is an excellent alternative for modeling irregular meshes, particularly those created by various computer-aided design/computer-aided manufacturing (CAD/CAM) systems (Neamah *et al.* 2022). This element, which has 10 nodes with three degrees of freedom each and translation in the nodal x and y directions, exhibits quadratic displacement behavior. The numerical approach is finished by meshing these beams after selecting the element type, as shown in Fig. 3d. The suitable element size was used depending on the convergence criteria (Saddam *et al.* 2024; Zainab *et al.* 2023, 2024).

For more details of simulation, the composite layer consists of one layer of fiberglass and two symmetrical epoxy layers. Thickness of composite beam (t_{Beam}) is 4 mm, while, the thickness of fiberglass layer (t_{Fiber}) is 0.7 mm. The thickness of epoxy layers (t_{Epoxy}) is calculated using the Eq. 4:

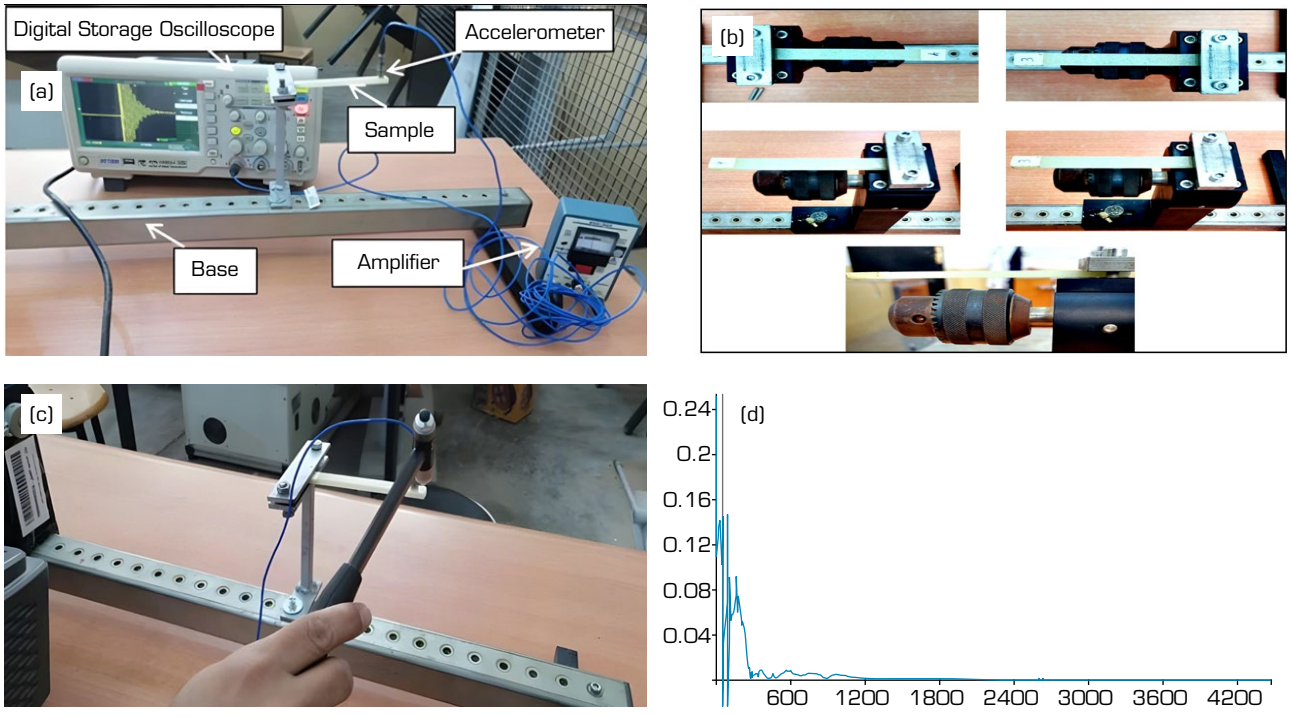

Source: Elaborated by the authors.

Figure 2. Beam samples under free vibration test. (a) free vibration test; (b) supporting type; (c) impact hummer; (d) FFT.

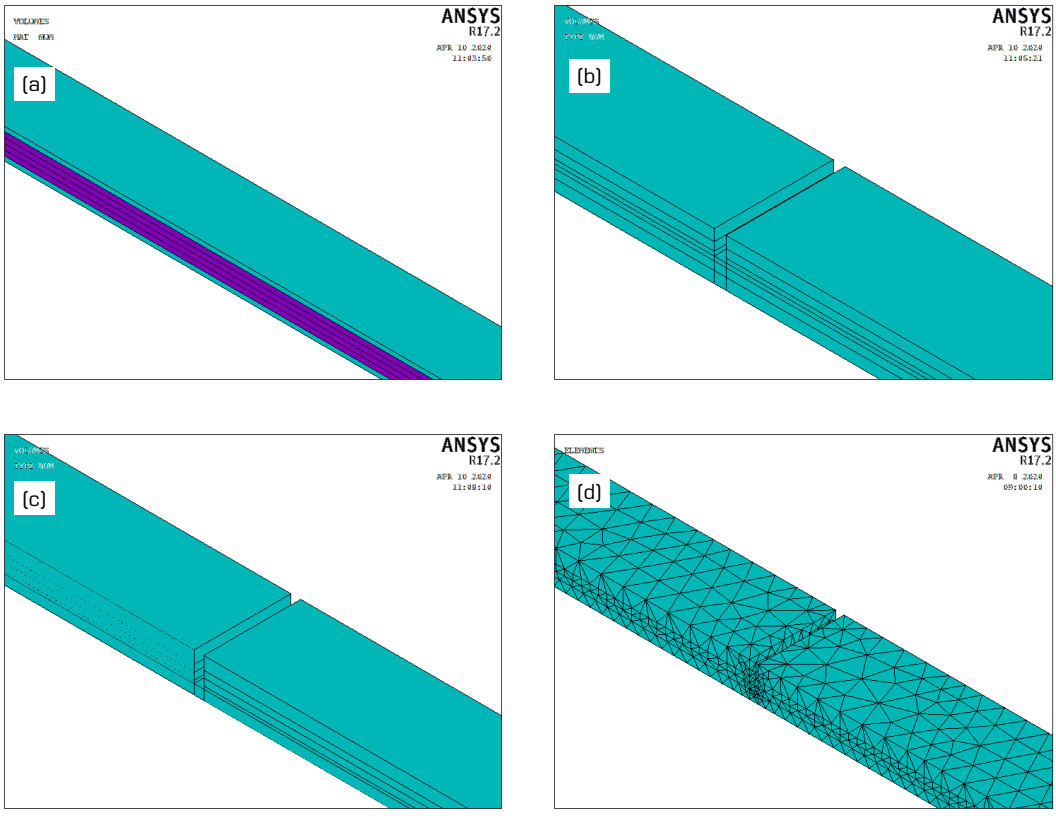

Source: Elaborated by the authors.

Figure 3. Numerical models of a composite beam with crack. (a) four-layers composite beam without crack; (b) three-layers composite beam with 2 mm crack; (c) two-layers composite beam with 3 mm crack; (d) meshing of cracked beam with 3 mm crack.

$$t_{Epoxy} = \frac{t_{Beam} - (n * t_{Fiber})}{2n} \quad (4)$$

In Table 3, epoxy thickness at different number of fiberglass layers is listed, and Fig. 4 shows the arrangement of these layers in composite beam.

Table 3. Thickness of epoxy layers depending on the number of layers.

No.	Thickness of beam (mm)	Thickness of fiberglass layer (mm)	Layers (n)	Thickness of epoxy layer (mm)
1	4	0.7	1	1.650
2	4	0.7	2	0.650
3	4	0.7	3	0.317
4	4	0.7	4	0.150

Source: Elaborated by the authors.

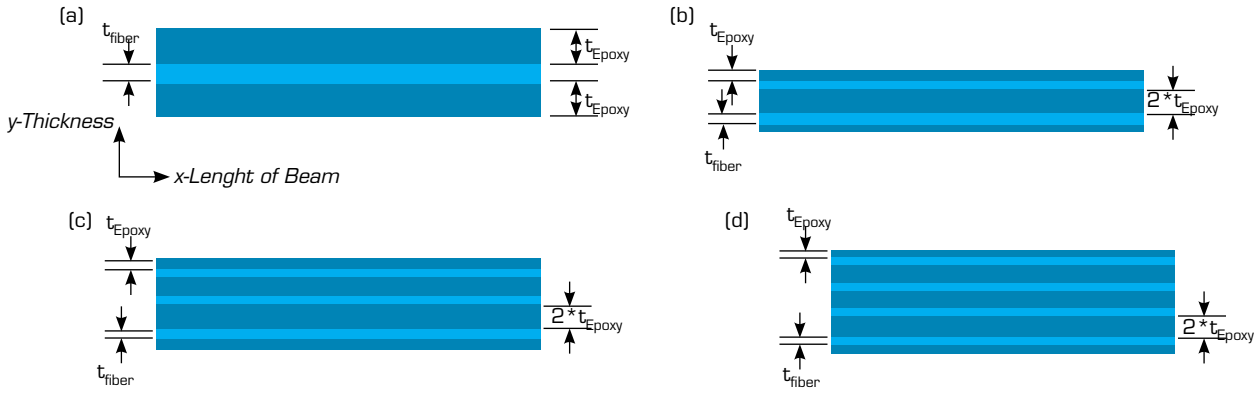

Source: Elaborated by the authors.

Figure 4. The arrangements of composite layers for different composite beams. (a) one-layer arrangement; (b) two-layers arrangement; (c) three-layers arrangement; (d) four-layers arrangement.

RESULTS AND DISCUSSIONS

Validation of the numerical method

The created composite beams were subjected to a free vibration test in order to determine their natural frequencies experimentally and increase the validity of the numerical work. The influence of cracking depth with different fiberglass layers was investigated while the boundary condition was C-F. Figure 5 and Table 4 depict the comparison of numerical and experimental work. Figure 5 shows that the numerical and experimental works are consistent with a 15% error rate ($Error\ \% = \frac{(f_{Num} - f_{Exp})}{f_{Num}} * 100$).

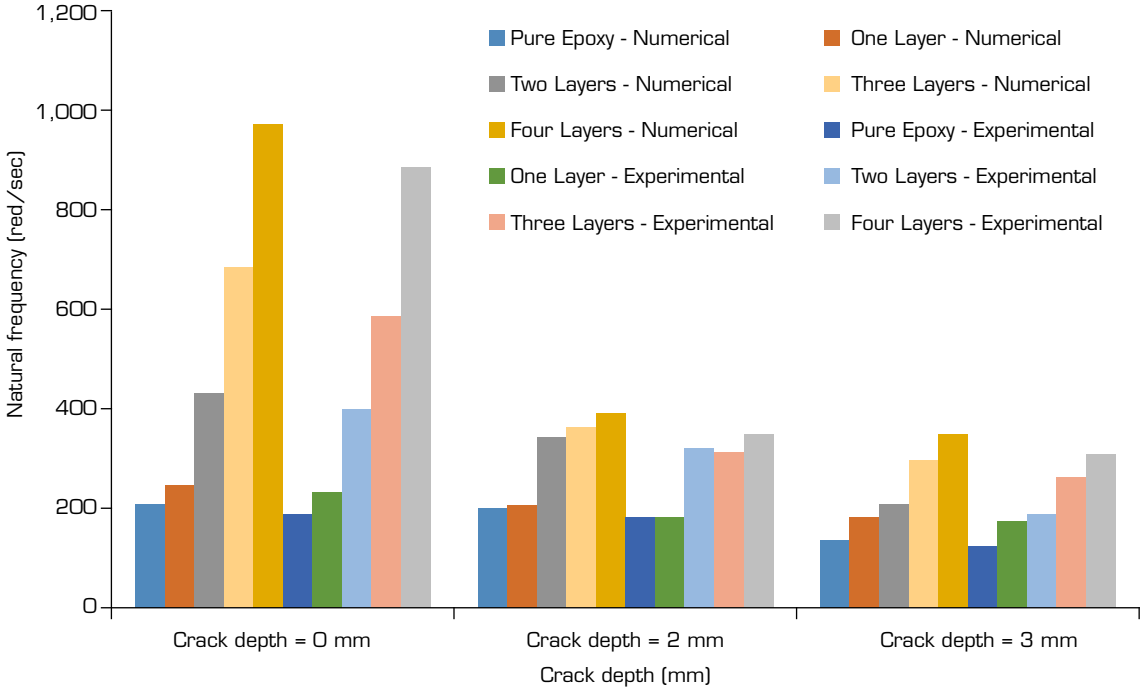

Source: Elaborated by the authors.

Figure 5. The comparison between the numerical and experimental works.

Table 4. Error percentage of the natural frequencies comparison between experimental and numerical results.

Type	Crack depth (mm)	Frequency (Hz)		Error %	Frequency (Hz)		Error %
		Numerical	Experimental		Numerical	Experimental	
		Pure epoxy			One-layer composite		
C-F	0	207.711	187.711	9.629	246.176	231.176	6.093
	2	200.545	185.545	7.480	205.249	188.000	8.404
	3	137.095	119.095	13.130	185.348	170.348	8.093
S-S	0	578.118	501.118	13.319	769.551	714.551	7.147
	2	511.512	466.512	8.797	634.028	599.028	5.520
	3	204.376	174.376	14.679	337.324	292.324	13.340
C-C	0	1,329.915	1,274.915	4.136	1,631.667	1,586.667	2.758
	2	1,300.023	1,265.023	2.692	1,583.502	1,517.502	4.168
	3	1,189.620	1,143.620	3.867	1,510.340	1,458.34	3.443
		Two-layers composite			Three-layers composite		
C-F	0	433.904	398.904	8.066	685.399	590.399	13.861
	2	342.850	320.000	6.665	366.281	316.281	13.651
	3	208.081	188.081	9.612	298.915	268.915	10.036
S-S	0	1,262.908	1,217.908	3.563	1,917.158	1,847.158	3.651
	2	1,043.818	974.818	6.610	1,286.081	1,201.081	6.609
	3	347.748	322.748	7.189	467.74	419.74	10.262
C-C	0	3,096.416	3,021.416	2.422	4,500.938	4,398.938	2.266
	2	2,311.655	2,237.655	3.201	2,350.384	2,250.384	4.255
	3	1,660.928	1,594.928	3.974	1,843.808	1,740.808	5.586
		Four-layers composite					
C-F	0	975.033	890.033	8.718			
	2	395.671	350.671	11.373			
	3	355.542	310.542	12.657			
S-S	0	2,727.843	2,637.843	3.299			
	2	1,419.594	1,328.594	6.410			
	3	968.564	874.564	9.705			
C-C	0	6,315.796	6,210.796	1.662			
	2	2895.960	2,780.960	3.971			
	3	2,296.658	2,188.658	4.702			

Source: Elaborated by the authors.

Numerical results

Effect of boundary conditions with different fiberglass layers

Figure 6 illustrates the effect of boundary conditions on the natural frequencies of complete beams with varying numbers of fiberglass layers. This Fig. shows that increasing the number of fiberglass layers one, two, three, and four layers increases natural frequency by 18.5, 108.9, 230, and 369.4% for the C-F support, 33.1, 118.4, 231.6, and 371.8% for the S-S beam, and 22.7, 132.8, 238.4, and 374.9% for the clamped-clamped (C-C) beam as listed in Table 5, where the increasing percentage (%) were calculated using the Eq. 5:

$$(Increasing\ Percentage)_{i-layer}\ (\%) = \frac{(f_{i-layer} - f_{Epoxy})}{f_{Epoxy}} * 100\% \quad (5)$$

where: $f_{i\text{-}layer}$ is the natural frequency of i-th composite beam (i = 1, 2, 3, and 4) and f_{Epoxy} is the natural frequency of epoxy.

This is a result of the fact that raising the fiberglass layer increases the elastic modulus of the beam, which leads to an increase in natural frequency. Furthermore, the boundary condition has a large impact on natural frequency, and the C-C beam has the highest natural frequency value.

Table 5. Increasing percentage of the natural frequencies of composite beams with respect to pure epoxy beam.

Support type	Crack depth (mm)	One-layer	Two-layers	Three-layers	Four-layers
C-F	0	18.519	108.898	229.977	369.418
	2	2.346	70.959	82.643	97.298
	3	35.197	51.779	118.035	159.340
S-S	0	33.113	118.452	231.621	371.849
	2	23.952	104.065	151.427	177.529
	3	65.051	70.151	128.862	373.913
C-C	0	22.690	132.828	238.438	374.902
	2	21.806	77.816	80.796	122.762
	3	26.960	39.618	54.991	93.058

Source: Elaborated by the authors.

Effect of crack depth on fiberglass layers and boundary conditions

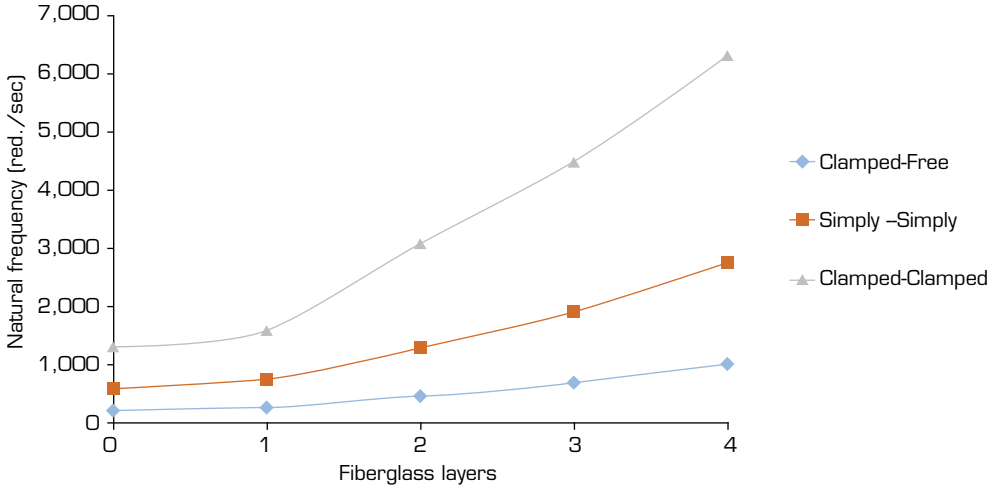

Source: Elaborated by the authors.

Figure 6. The effect of boundary condition with different fiberglass layers.

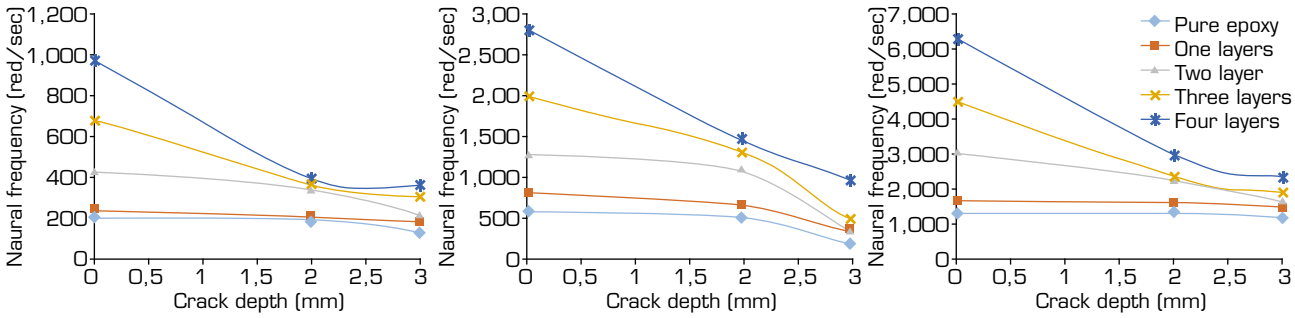

Source: Elaborated by the authors.

Figure 7. The frequency of cracked composite beam with different boundary conditions: (a) C-F; (b) simply support; (c) C-C.

Figure 7 depicts the influence of crack depth on the free vibration of this beam with various boundary conditions and fiberglass layers. Based on this graph, it is possible to assume that, as cracking depth increases, the natural frequency decreases. This is because the effective elastic modulus of a developed beam decreases with increasing cracking depth, causing the natural frequency to decrease. Furthermore, the influence of crack depth on reducing the natural frequency value of the composite beam increases as the number of fiberglass layers increases.

The first mode shape

The first mode form of a composite beam is demonstrated for various crack depths, fiberglass layers, and boundary conditions. Figures 8-16 show the first mode for various composite beams with C-F, simply-simply, and C-C boundary conditions. From Fig. 7, the first mode of a C-F composite varies with increasing the crack depth and this appears sharply by increasing (a) the maximum deflection, (b) the region of minimum deflection (blue region), and (c) the region of minimum deflection (red region). On the other hand, the maximum deflection decreases when the number of layers increases because of the increasing the equivalent modulus of elasticity of the C-F composite beam. Similar observations can be seen in Figs. 9 and 10 for the first mode of S-S and C-C composite beams, respectively. However, the impact of crack depth for S-S and C-C composite beams is greater than that for C-F composite beams because 1) in S-S and C-C composite beams, the crack lies in the position of maximum deflection, whereas

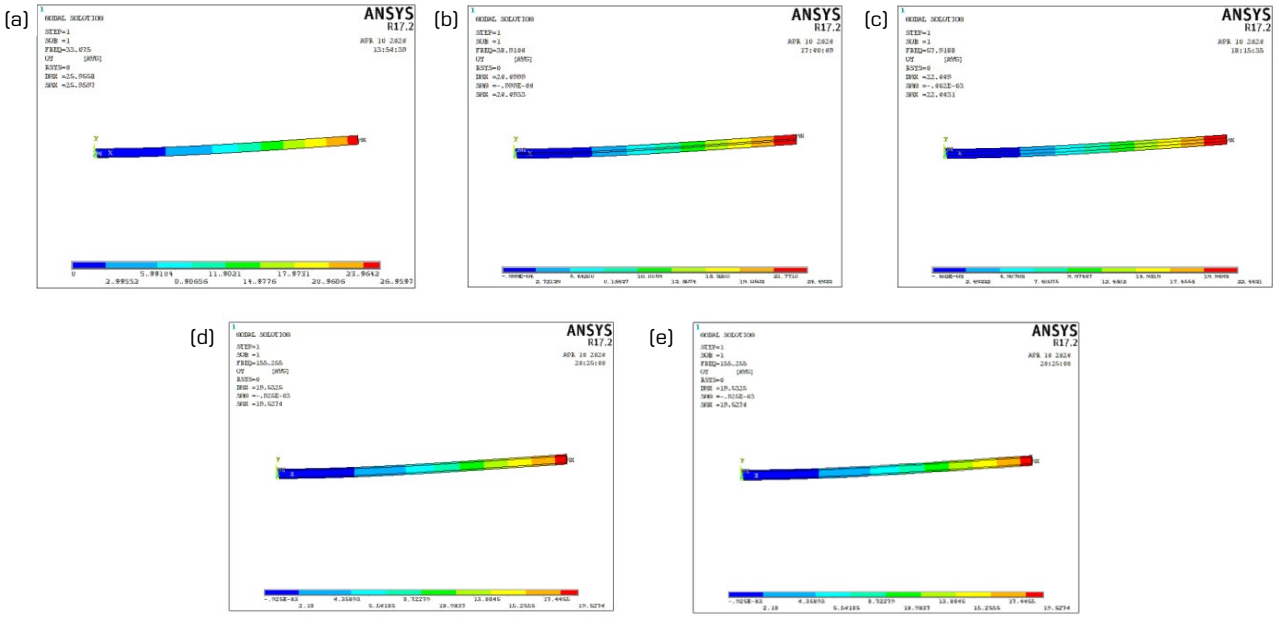

Source: Elaborated by the authors.

Figure 8. The first mode shape of C-F composite beam without crack. (a) pure epoxy; (b) one-layer composite; (c) two-layers composite; (d) three-layers composite; (e) four-layers composite.

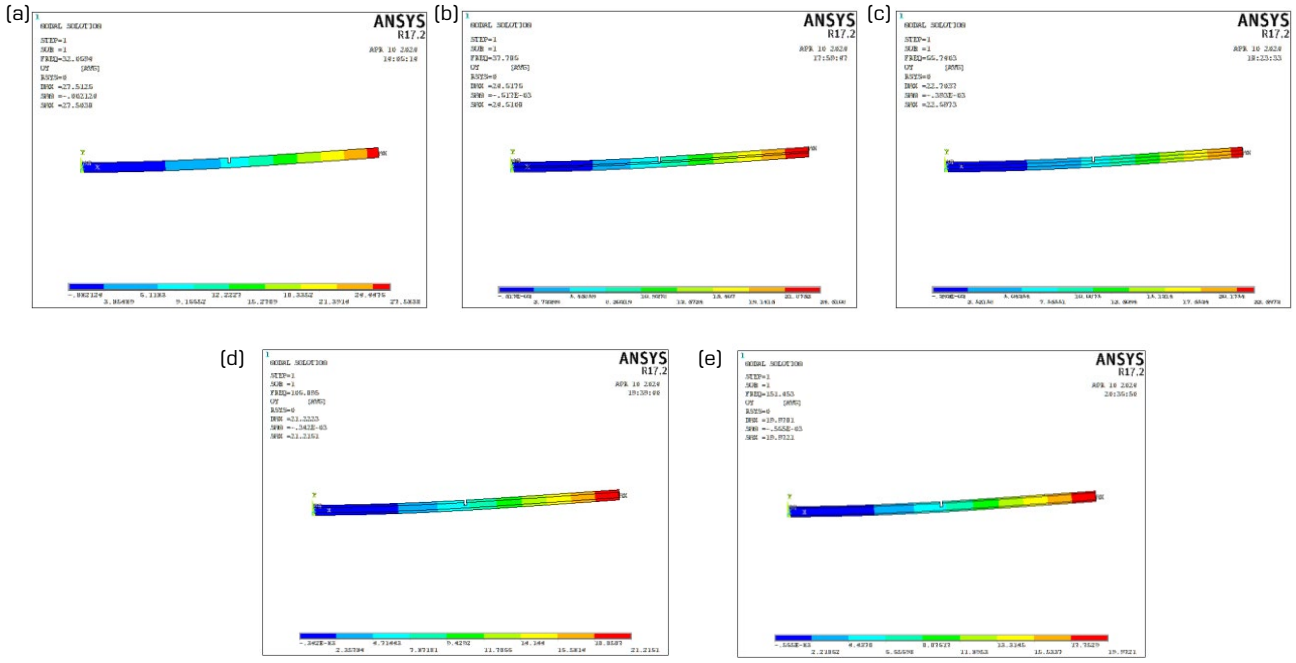

Source: Elaborated by the authors.

Figure 9. The first mode shape of C-F composite beam with (2 mm) crack. (a) pure epoxy; (b) one-layer composite; (c) two-layers composite; (d) three-layers composite; (e) four-layers composite.

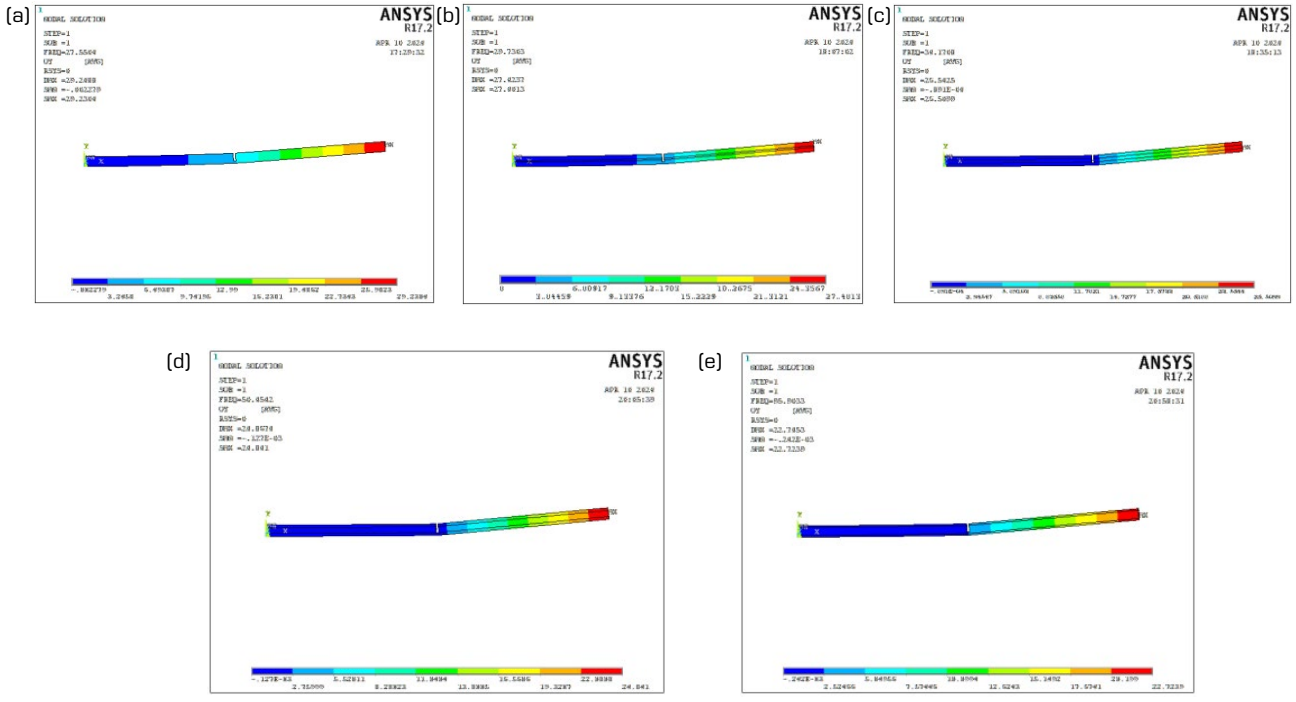

Source: Elaborated by the authors.

Figure 10. The first mode shape of C-F composite beam with (3 mm) crack. (a) pure epoxy; (b) one-layer composite; (c) two-layers composite; (d) three-layers composite; (e) four-layers composite.

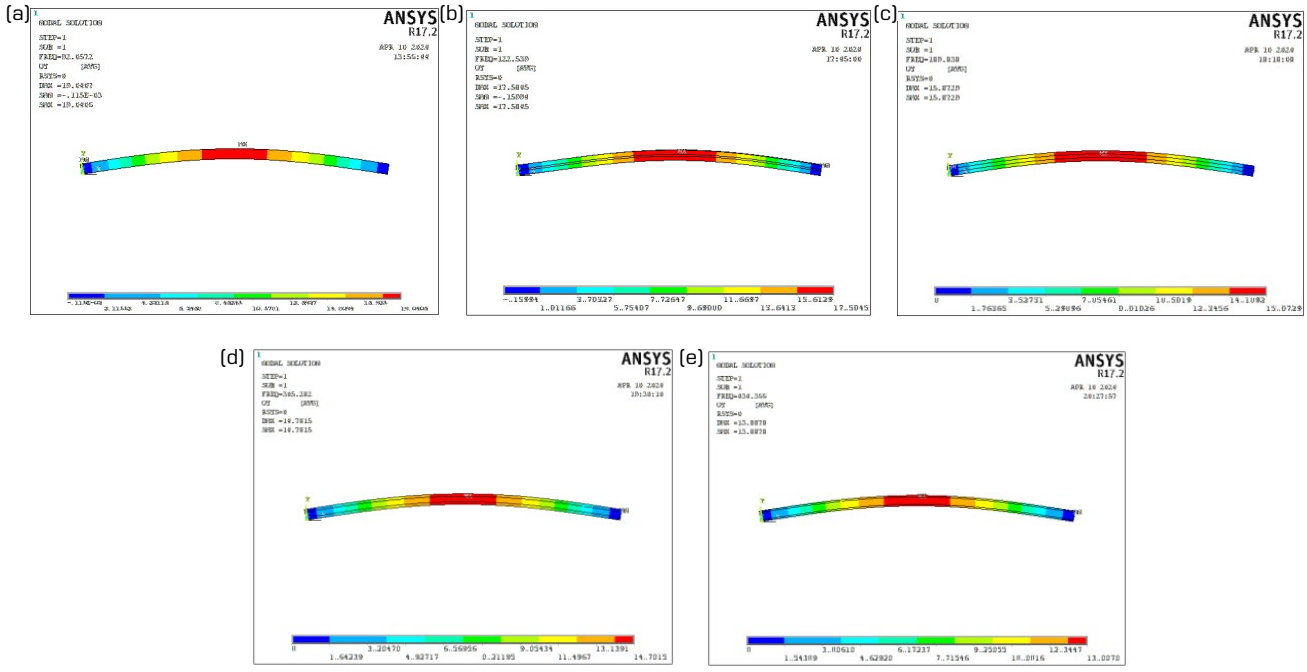

Source: Elaborated by the authors.

Figure 11. The first mode shape of S-S composite beam without crack. (a) pure epoxy; (b) one-layer composite; (c) two-layers composite; (d) three-layers composite; (e) four-layers composite.

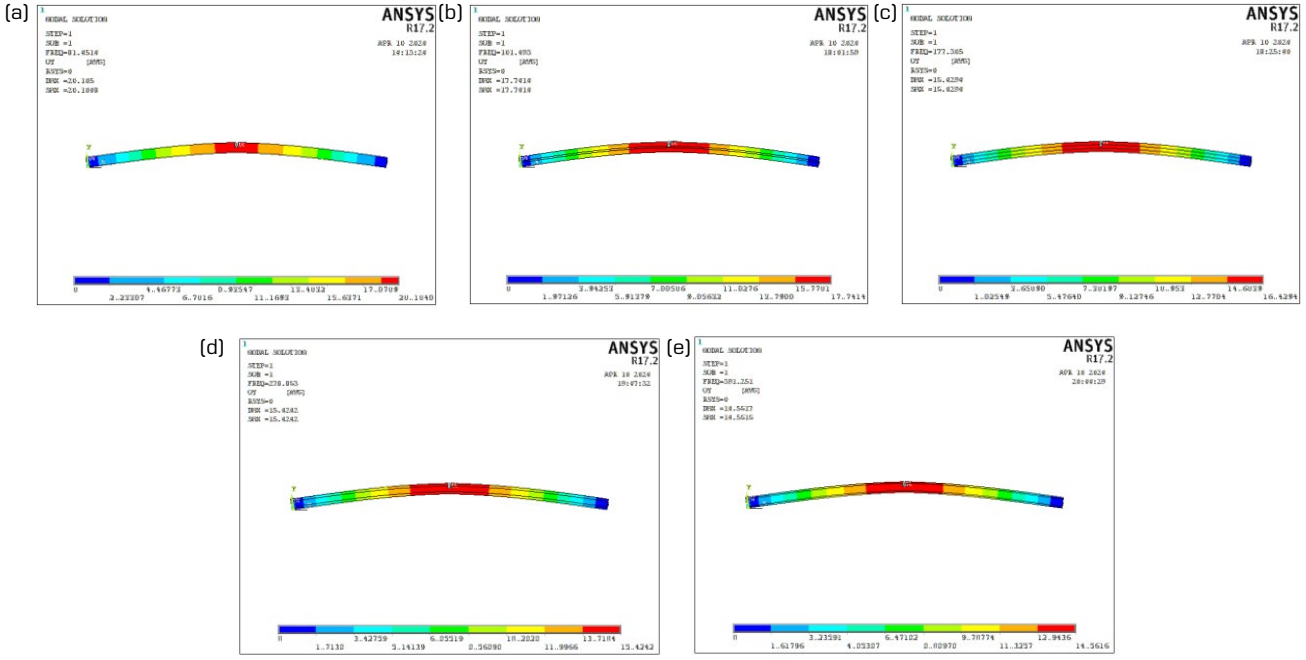

Source: Elaborated by the authors.

Figure 12. The first mode shape of S-S composite beam with (2 mm) crack. (a) pure epoxy; (b) one-layer composite; (c) two-layers composite; (d) three-layers composite; (e) four-layers composite.

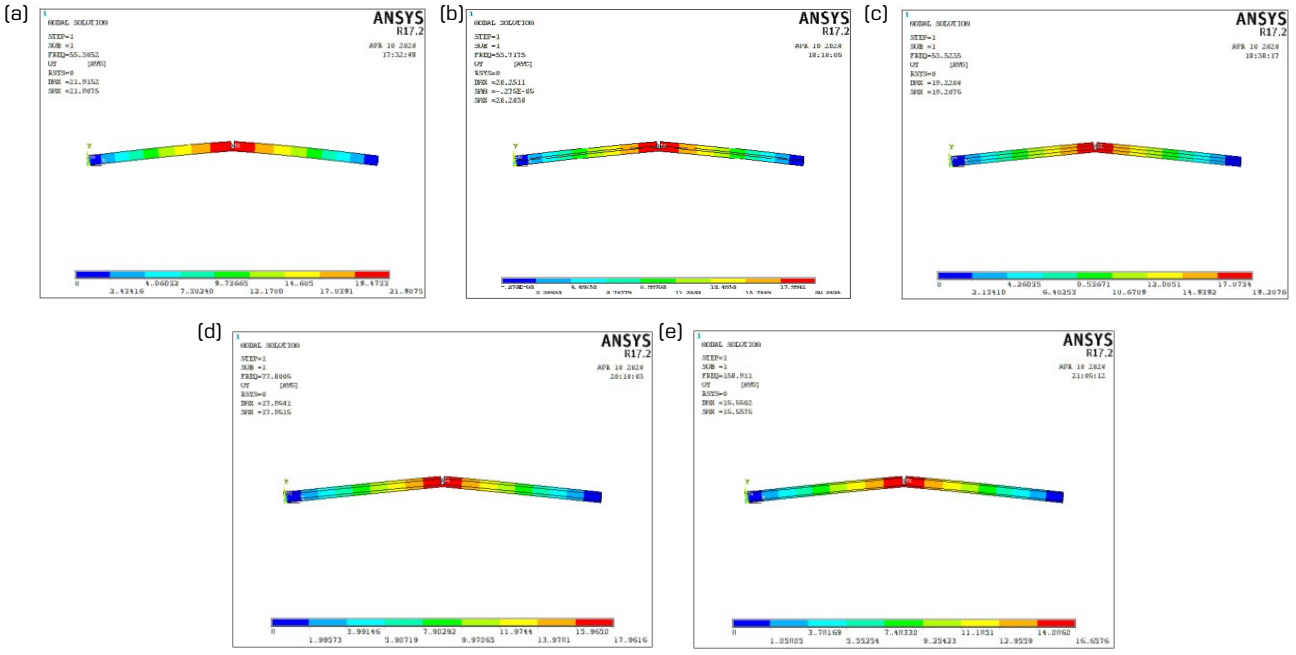

Source: Elaborated by the authors.

Figure 13. The first mode shape of S-S composite beam with (3 mm) crack. (a) pure epoxy; (b) one-layer composite; (c) two-layers composite; (d) three-layers composite; (e) four-layers composite.

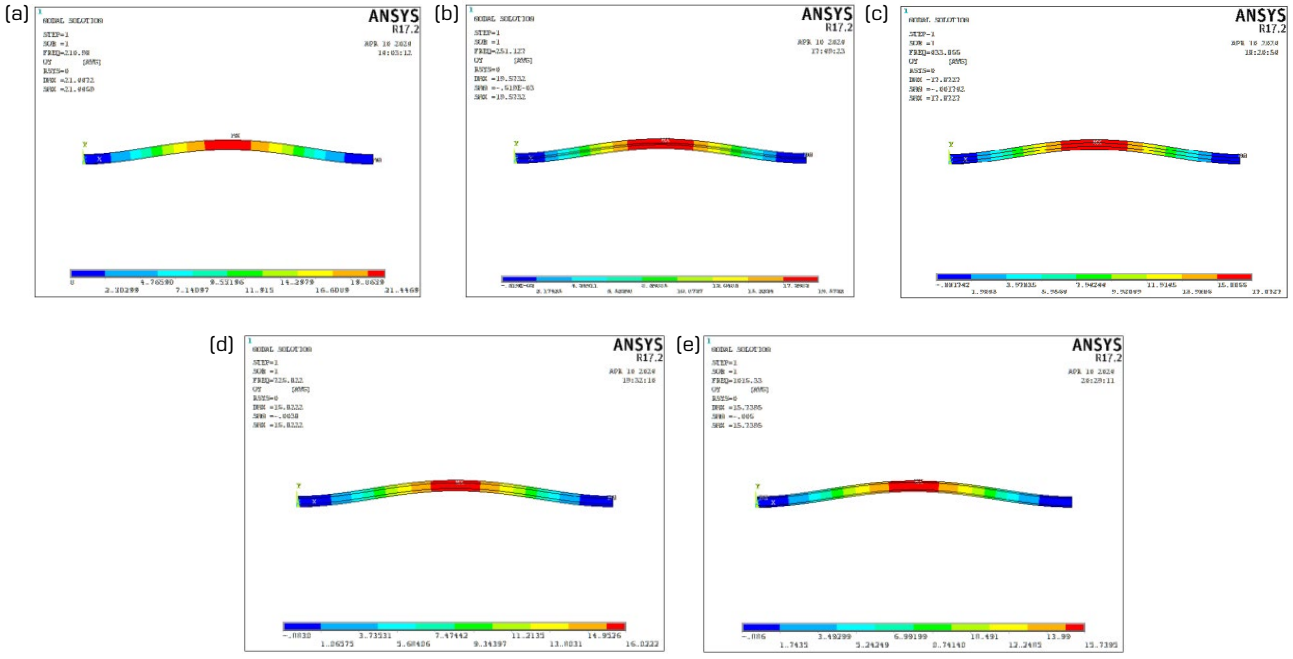

Source: Elaborated by the authors.

Figure 14. The first mode shape of C-C composite beam without crack. (a) pure epoxy; (b) one-layer composite; (c) two-layers composite; (d) three-layers composite; (e) four-layers composite.

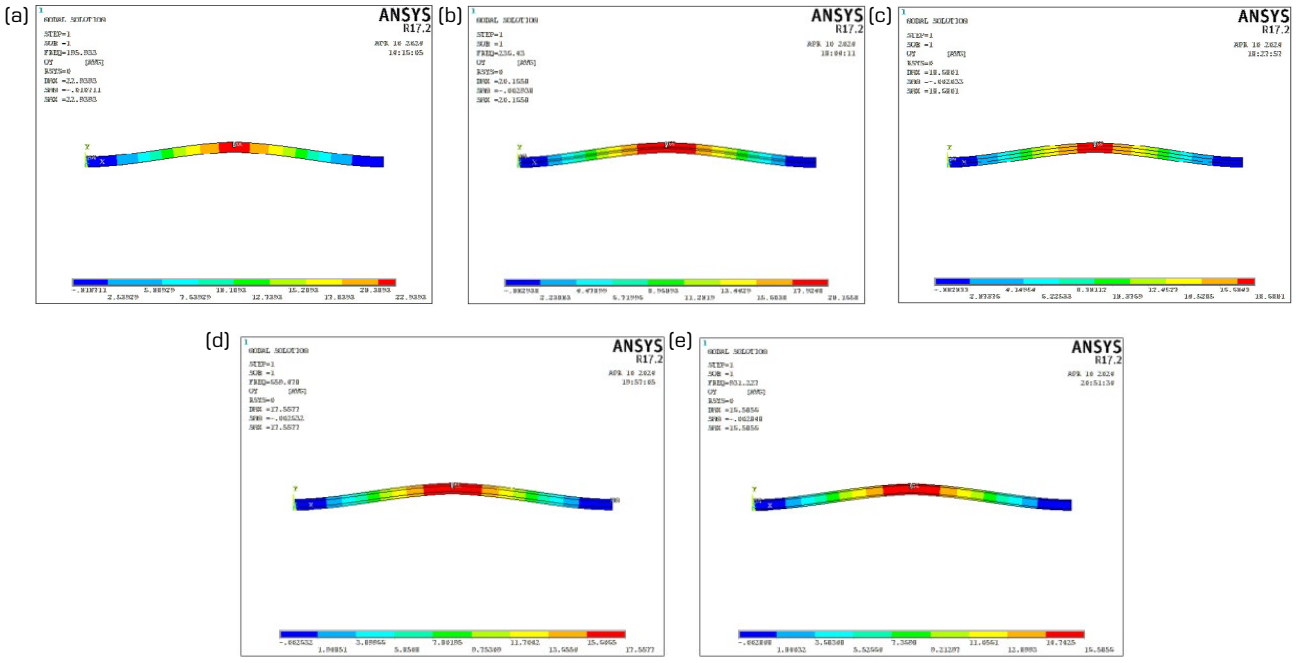

Source: Elaborated by the autors.

Figure 15. The first mode shape of C-C composite beam with (2 mm) crack. (a) pure epoxy; (b) one-layer composite; (c) two-layers composite; (d) three-layers composite; (e) four-layers composite.

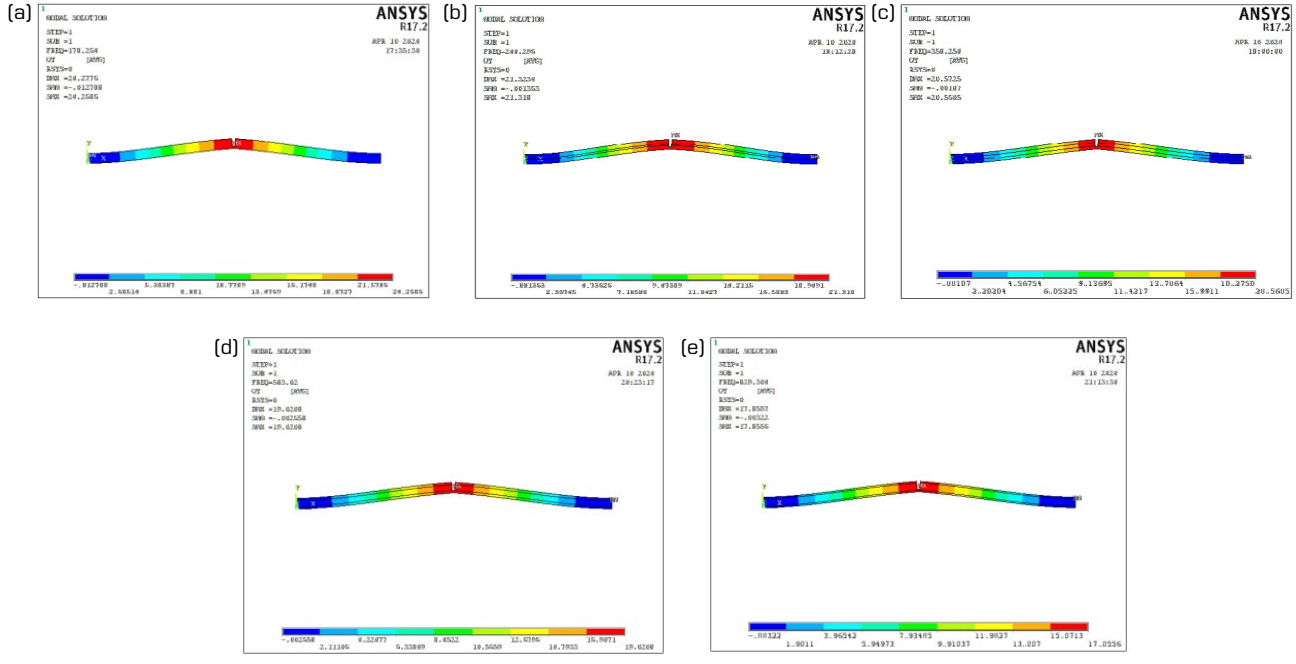

Source: Elaborated by the authors.

Figure 16. The first mode shape of C-C composite beam with (3 mm) crack. (a) pure epoxy; (b) one-layer composite; (c) two-layers composite; (d) three-layers composite; (e) four-layers composite.

the crack does not lie in the position of maximum deflection in C-F composite beams, 2) generally, the frequency of C-F beams is smaller than that of S-S and C-C beams, respectively, for the same dimensions and properties of beams and 3) the deflection of C-F beams is greater than that of S-S and C-C beams, respectively, for the same dimensions and properties of beams.

CONCLUSION

The effects of fracture depth, number of fiberglass layers, and boundary conditions on the natural frequency and mode shape of the composite beam were investigated using numerical and experimental approaches. The number of fiberglass layers was determined by calculating volume fractions. From the current work, the following conclusions are drawn:

- The numerical model is adequate since the variation between it and the experimental work is less than 15%.
- It was discovered that increasing the number of fiberglass layers increases the natural frequency.
- As the crack depth increases, the frequency decreases due to decreased stiffness of the composite beam.
- As the number of fiberglass layers rises, the influence of the crack's depth on the natural frequency value of the composite beam increases.
- The impact of crack depth for S-S and C-C composite beams is greater than that for C-F composite beams
- Vibration signals can be used to diagnose a cracked structure.

CONFLICT OF INTEREST

Nothing to declare.

AUTHORS' CONTRIBUTION

Conceptualization: Neamah RA; **Methodology:** Neamah RA and Njim EK**; Software** Neamah RA and Al-Ansari LS**; Validation:** Neamah RA and Al-Raheem SK**; Formal analysis:** Neamah RA and Abboud Z**; Investigation:** Neamah RA and Abboud Z**; Resources:** Neamah RA and Al-Raheem SK**; Data curation:** Neamah RA and Al-Ansari LS**; Writing - Original draft:** Neamah RA; **Writing - Review & Editing:** Neamah RA and Njim EK**; Visualization:** Neamah RA and Njim EK; **Supervision:** Neamah RA and Al-Ansari LS**; Project administration:** Neamah RA and Al-Ansari LS**; Funding acquisition:** Neamah RA and Al-Raheem SK; **Final approval:** Neamah RA.

DATA AVAILABILITY STATEMENT

All data sets were generated or analyzed in the current study.

FUNDING

Not applicable.

ACKNOWLEDGMENTS

Not applicable.

REFERENCES

Daneshmehr A, Nateghi A, Inman D (2013) Free vibration analysis of cracked composite beams subjected to coupled bending-torsion loads based on a first order shear deformation theory. Appl Math Model 37(4):10074-10091. https://doi.org/10.1016/j.apm.2013.05.062

Das P, Sahu SK (2020) Experimental and numerical study on free vibration of cracked woven fiber glass/epoxy composite beam. Mater Today Proc 33(8):5505-5510. https://doi.org/10.1016/j.matpr.2020.03.320

Dipen KR, Pratiksha HW, Emanoil L (2021) Manufacturing technologies of carbon/glass fiber-reinforced polymer composites and their properties: a review. Polymers 13(21):3721. http://doi.org/10.3390/polym13213721

Du H, Yuan S, Yu T, Hu X (2023) Experimental and analytical investigation on flexural behavior of high-strength steel-concrete composite beams. Buildings 13(4):902. https://doi.org/10.3390/buildings13040902

Gay D (2022) Composite materials: design and applications. Boca Raton: CRC Press.

Hu Z, Ni Z, An D, Chen Y, Li R (2023) Hamiltonian system-based analytical solutions for the free vibration of edge-cracked thick rectangular plates. Appl Math Model 117:451-478. https://doi.org/10.1016/j.apm.2022.12.036

Jena PC, Parhi DR, Pohit G (2014) Theoretical, numerical (FEM) and experimental analysis of composite cracked beams of different boundary conditions using vibration mode shape curvatures. Int J Eng Technol 6(2):509-518.

Kahya V, Karaca S, Okur FY, Altunışık AC, Aslan M (2019) Free vibrations of laminated composite beams with multiple edge cracks: numerical model and experimental validation. Int J Mech Sci 159:30-42. https://doi.org/10.1016/j.ijmecsci.2019.05.032

Kahya V, Karaca S, Okur FY, Altunışık AC, Aslan M (2021) Damage localization in laminated composite beams with multiple edge cracks based on vibration measurements. IJST-T Civ Eng 45:75-87. http://doi.org/10.1007/s40996-020-00393-x

Kim K, Choe K, Kim S, Wang Q (2019) A modeling method for vibration analysis of cracked laminated composite beam of uniform rectangular cross-section with arbitrary boundary condition. Compos Struct 208:127-140. https://doi.org/10.1016/j.compstruct.2018.10.006

Libo Y, Nawawi C, Krishnan J (2014) Flax fibre and its composites – A review. Composites Part B: Engineering 56:296-317. http://doi.org/10.1016/j.compositesb.2013.08.014

Naskar S, Mukhopadhyay T, Sriramula S, Adhikari S (2017) Stochastic natural frequency analysis of damaged thin-walled laminated composite beams with uncertainty in micromechanical properties. Compos Struct 160:312-334. https://doi.org/10.1016/j.compstruct.2016.10.035

Neamah RA, Nassar AA, Alansari LS (2022) Modeling and analyzing the free vibration of simply supported functionally graded beam. J Aerosp Technol Manag 14:1-26. http://doi.org/10.1590/jatm.v14.1257

Orhan S, Lüy M, Dirikolu M, Zorlu G (2016) The effect of crack geometry on the nondestructive fault detection in a composite beam. International Journal of Acoustics and Vibrations 21(3). http://doi.org/10.20855/ijav.2016.21.3420

Priyadarshi D, Manoj KM, Sasanka C, Nibedita P, Bidyadhar B, Shishir KS (2024) A concerted experimental and numerical approach for frequency based non-destructive analysis of bi-directional cracked laminated composite beams. Nondestruct Test Eva 1:1-26. http://doi.org/10.1080/10589759.2024.2304270

Priyadarshi D, Shishir KS (2021) Free vibration analysis of industry-driven woven fiber laminated carbon/epoxy composite beams by experimental and numerical approach. Polym Polym Compos 29(9S):S1371-S1385. http://doi.org/10.1177/09673911211052825

Priyadarshi D, Shishir KS (2022) Experimental and numerical free vibration analysis of industry-driven woven fibre laminated glass/epoxy composite beams. Curr Sci 122(9):1058. http://doi.org/10.18520/cs/v122/i9/1058-1065

Priyadarshi D, Manoj KM, Shishir KS (2021) On crack detection in a laminated glass/epoxy composite beam under free vibration with fuzzy logic aid. Int J Struct Stab Dyn 21(13):2150176. http://doi.org/10.1142/S0219455421501765

Reddy KM, Vardhan DH, Reddy YSK, Gujjala R, Ramesh R (2021) Experimental study of thermal and mechanical behaviour of graphite-filled UJF composite. Adv Maters Sci Eng e3739573:1-7. http://doi.org/10.1155/2021/3739573

Saddam KA, Hayder ZZ, Aziz DA, Alansari LS, Saif WMA (2024) Static deflection of pre-twisted beam subjected to transverse load. Results Eng 21:e101953. http://doi.org/10.1016/j.rineng.2024.101953

Sahu SK, Das P (2020) Experimental and numerical studies on vibration of laminated composite beam with transverse multiple cracks. Mech Syst Signal Process 135:e106398. https://doi.org/10.1016/j.ymssp.2019.106398

Sanjay MR, Arpitha GR, Yogesha B (2014) Investigation on mechanical property evaluation of jute-glass fiber reinforced polyester. IOSR Journal of Mechanical and Civil Engineering 11(4):50-57. http://doi.org/10.9790/1684-11455057

Shareef MM, Al-Khazraji AN, Amin SA (2021) Flexural properties of functionally graded polymer alumina nanoparticles. Eng Technol 39(5A):821-835. https://doi.org/10.30684/etj.v39i5A.1949

Suriani MJ, Ilyas RA, Zuhri MYM, Khalina A, Sultan MTH, Sapuan SM, Ruzaidi CM, Wan FN, Zulkifli F, Harussani MM, et al. (2021) Critical review of natural fiber reinforced hybrid composites: processing, properties, applications and cost. Polymers 13(20). http://doi.org/10.3390/polym13203514

Tri-Dung N (2020) Composite and nanocomposite materials – From knowledge to industrial applications. Rijeka: IntechOpen. http://doi.org/10.5772/intechopen.91285

Weronika G, Szymon R, Marcin P, Beata D (2023) Effect of modification of flax fibers with silanes and polysiloxanes on the properties of PLA-based composites. J Nat Fibers 20(2). http://doi.org/10.1080/15440478.2023.2280042

Zainab MS, Raghad AN, Husam JA, Al-Ansari LS, Sutartip W (2024) Calculating the natural frequency of pre-twisted beam. J Eng Sustain Dev 28(1). http://doi.org/10.31272/jeasd.28.1.1

Zainab MS, Raisan FH, Yassar KA, Al-Ansari LS, Mohammedh H (2023) Investigating the effect of applying uniform distributed load on the deflection of simply supported axial – Functionally graded beam. J Aerosp Technol Manag 15:e2423. http://doi.org/10.1590/jatm.v15.1315

Zou Y, Yu K, Heng J, Zhang Z, Peng H, Wu C, Wang X (2023) Feasibility study of new GFRP grid web – Concrete composite beam. Compos Struct 305:e116527. https://doi.org/10.1016/j.compstruct.2022.116527